Journal of Engineering Science and Technology
Vol. 21, No. 3 (2026) 836 - 853


# EXPLORATORY STUDY ON USING HYBRID POLYPROPYLENE FIBERS WITH SLAG AGGREGATE TO MITIGATE CRACKS IN RC BRIDGE SLABS

WALEED K. HAMID[1,*], HUSAM H. HUSSEIN[2], NABEEL A. FARHAN[3], FOUAD AL RIKABI[4], ISSAM KHOURY[5]

[1]Department of Construction and Projects, University of Fallujah, 31002, Fallujah, Iraq
[2]Senior Project Manager at GFT, 43004, Columbus, Ohio, USA
[3]Department of Construction and Projects, University of Fallujah, 31002, Fallujah, Iraq
[4]Senior Roadway Engineer at AECOM, Powell, 43065, Ohio, USA
[5]Dept. of Civil Engineering, Ohio University, Athens, Ohio, USA
*Corresponding Author: Dr.Waleed.Hamid@uofallujah.edu.iq

## Abstract

Slag aggregate concrete has been employed to reduce crack development in reinforced concrete bridge slabs and to contribute to sustainability by reducing the environmental impact of the construction industry. The addition of polypropylene (PP) fibres to slag aggregate concrete can improve its mechanical properties. Fiber length has a significant role in post-cracking behaviour. However, long PP fibres with low elastic modulus and small diameter are more prone to bending within the concrete slurry. Therefore, incorporating a blend of different PP fibre lengths (a hybrid fibre) in slag concrete mixtures is used to enhance the mechanical strength and durability of concrete. There is limited research investigating the influence of hybrid PP fibres with varying lengths on the mechanical properties of slag concrete, where coarse natural aggregate is fully replaced with coarse slag aggregate. A new method for testing tensile strength was developed in the current study. Based on the tested specimens, incorporating PP hybrid fibre with slag concrete exhibited a trend toward improved mechanical properties. It was also noted that the newly developed direct tension test minimizes stress eccentricity, thereby improving the reliability of the experimental outcomes. The inclusion of a high volume of long fibres in the mixture led to a trend toward improved ultimate strength, in terms of both tensile strength and toughness. The ultimate tensile strength and toughness increased by 17% and 21%, respectively, compared with control mix. The results of the modulus of elasticity and coefficient of thermal expansion of the slag concrete were also concluded. A good agreement was observed between the results from the ACI 318 equation and the experimental data. In addition, A finite element model of the bridge superstructure was used to investigate the overall behaviour of the bridge under gradient temperature effects. It was observed that fibre-reinforced mixtures experience higher tensile stresses under temperature gradients compared with plain concrete.

Keywords: Coefficient of thermal expansion, Hybrid PP fibres, New direct tension test, Slag aggregate, Toughness.

## 1. Introduction

The potential cracking of bridge decks at an early age is the main factor affecting the long-term performance of bridge decks. Concrete shrinkage, thermal effects, and external loadings caused the cracks. These cracks directly allow chloride ions to penetrate the decks and then corrode the reinforcement. Consequently, the bridge's service life will be reduced [1, 2]. These concrete deck cracks are generated when the tensile strength of the concrete is lower than the tensile stress [3, 4]. Therefore, it is crucial to mitigate early-age cracking by minimizing shrinkage and thermal effects. This behaviour can be achieved using durable concrete [5]. Numerous factors affect the durability of concrete, which were defined by the National Cooperative Highway Research Program (NCHRP 380) [6].

One of these factors is the aggregate type. Neville [7] showed that concrete with higher-stiffness aggregates tends to experience higher shrinkage than concrete containing aggregates with lower stiffness. Therefore, Slag aggregates are suggested for use in concrete decks to mitigate the development of cracks [8]. Slag aggregates possess a high porosity and absorbency compared to natural aggregates. This water absorption process enables them to function as a source of internal curing, where water retained in their pores is gradually released during the hydration of the cement. This process can eliminate shrinkage, particularly in concrete mixtures with a low water-to-cement ratio [4, 8, 9].

The primary objective of using slag aggregate in concrete mixtures is to mitigate concrete cracking in bridge decks and enhance the environment by reducing the industry's environmental impact. Steel slag is one of the types of slag aggregate formed in the blast furnace during cast iron production. The steel industry removes waste from the furnace, accounting for approximately 10-15% of the total steel produced [10]. The annual slag production worldwide was approximately 280 million tons in 2019 [11]. Therefore, using steel slag in concrete applications will minimize its environmental impact and promote environmental sustainability [12].

Incorporating polypropylene (PP) fibres with slag aggregates can enhance the mechanical properties of concrete [13] and improve its resistance to potential cracking [14]. The improvement in these properties depended on the effect of the fibre’s size, length, and dosage [13, 15]. Al Rikabi et al. [16] showed that the fibre content or fibre length significantly influences post-cracking behaviour. They concluded that longer fibres or higher fibre content had more embedded length than the other dosages, resulting in higher post-cracking. However, other research showed that increasing the length of PP fibres had an inverse effect on the compressive strength of concrete. This was because the PP fibres bent during the concrete mixing process, which reduced their effective length [17].

Concrete failure occurs across multiple stages, beginning with the initiation and development of microcracks and then extending to the formation of macrocracks. Microfibers with small diameters and large aspect ratios have a marked impact on the initiation and propagation of microcracks during loading. However, microfibers exhibit poor adhesion to the concrete paste, which can lead to the propagation of macrocracks [18]. In contrast, macrofibres, which have larger diameters and lengths, possess high bonding strength with the concrete paste and can effectively bridge the widening of macrocracks [19]. Therefore, concrete with a combination of micro and macro steel fibres can create a synergistic effect, enhancing its mechanical properties [20].

Numerous studies on hybrid fibre-reinforced concrete have been carried out, offering important insights and methods applicable to a variety of engineering applications. He et al. [20] investigated the influence of hybrid steel fibres on the mechanical properties of conventional concrete in terms of compressive strength, tensile strength, and flexural strength. They reported that hybrid fibre noticeably improved the tensile and flexure strength of concrete. Kinjawadekar et al. [21] studied the impact of incorporating different combinations of steel, basalt, and glass fibres into conventional concrete on its mechanical strength.

The study provided a comparative analysis of various fibre percentages to improve concrete properties and identifies the optimal fibre content among the proportions considered. Khan et al. [22] evaluated the effect of incorporating different combinations of steel and polypropylene fibres into conventional concrete on its mechanical strength. The results showed notable increases in compressive strength and split tensile strength relative to the control samples without fibres. The study provided valuable insights into the design and behaviour of hybrid fibre-reinforced concrete, offering a foundation for future research on its performance under dynamic loading conditions.

Further exploration and comprehensive evaluation are needed, particularly in optimizing mechanical characteristics of slag concrete, which are essential for the performance of load-carrying concrete structures. Therefore, the current study aims to evaluate the effect of replacing 100% of the coarse natural aggregate with slag aggregate on the mechanical properties of concrete. Previous studies relied on a specific PP fibre length in each mix; however, the current research used a blend of different PP fibre lengths (a hybrid fibre).

Using only one length of fibre often results in performance constraints, as no single length of fibre possesses ideal mechanical properties. Fiber length plays a crucial role in post-cracking performance. Longer fibres provide stronger bonding and exhibit improved behaviour after cracking compared to shorter ones [16]. However, long PP fibres are more prone to bending within the concrete slurry due to their low elastic modulus and small diameter [17, 23]. Thus, hybrid fibres are incorporated to enhance the mechanical strength and durability of concrete. Incorporating hybrid PP fibre with steel aggregate concrete was also evaluated. To achieve this goal, a new direct tensile strength method was developed to provide fundamental concrete properties.

## 2. Experimental Program

### 2.1. Materials and mix proportions

Three concrete mixes with a water/cement ratio (w/c) of 0.30 were tested to investigate the impact of incorporating hybrid PP fibre with steel slag aggregate on the tensile strength of concrete. All mixtures contained 100% steel slag aggregate with sizes of 4/20 mm, instead of coarse aggregate, and river sand as the fine aggregate, as shown in Fig. 1. The source of steel slag aggregate was an Electric Arc Furnace (EAF) in Ohio, USA. Monofilament PP fibres with a diameter of 40 μm were utilized. Fiber content of 1% by volume, with three different fibre lengths (19, 38, and 57 mm), was incorporated into the mix based on a previous study. Figure 2 shows the fibre length. The Young's modulus and tensile strength of the fibre were 4050 and 586 MPa, respectively.


**Fig. 1. Steel slag aggregate and river sand.**


**Fig. 2. PP fibre lengths.**

The specific gravity of the PP fibre was 0.92 g/cm³. The coefficient of thermal expansion of the fibre ranged from 70 to 100 x$10^{-6}$/°C. Table 1 presents the proportions of the concrete mixtures. Three series of slag aggregate concrete incorporating different types of hybrid PP fibres were designated as H1, H2, and H3, respectively. In addition, a control slag concrete mix without fibres, defined as C, was also included. The hybrid PP fibre consisted of three different lengths of PP fibre with a fibre content of 1% by volume. H1 mix consisted of 0.5% PP fibre with a length of 57 mm, 0.25% PP fibre with a length of 38 mm, and 0.25% PP fibre with a length of 19 mm. H2 mix included 0.25% PP fibre measuring 57 mm, along with 0.5% fibres of 38 mm and another 0.25% of 19 mm fibres.

**Table 1. Mix proportion of slag concrete.**

| Constituents | Amount |
|---|---|
| **Cement type I/II (kg/m³)** | 460 |
| **Fine Agg. (kg/m³)** | 750 |
| **EAF Coarse Agg. (kg/m³)** | 985 |
| **HWRA (L/m³)** | 2.75 |
| **Air Entrained (L/m³)** | 0.11 |
| **w/c ratio** | 0.30 |

H3 mix consisted of 0.25% PP fibre with a length of 57 mm, 0.25% PP fibre with a length of 38 mm, and 0.5% PP fibre with a length of 19 mm. Details of concrete mixes are presented in Table 2. The slag concrete constituents were blended carefully to avoid the formation of fibre clumps. Fibers were incorporated after all other ingredients had been mixed to ensure uniform distribution throughout the mixture. Following casting, the specimens were wrapped in a plastic sheet to preserve their moisture content. The specimens were demoulded 24 hours after casting and were immersed in water for 28 days.

**Table 2. Details of concrete mixes.**

| Mix ID | Fiber content per length, % | | | Total content, % |
|---|---|---|---|---|
| | 19 mm | 38 mm | 57 mm | |
| **C** | 0 | 0 | 0 | 0 |
| **H1-57-0.5%** | 0.25 | 0.25 | 0.5 | 1 |
| **H2-38-0.5%** | 0.25 | 0.50 | 0.25 | 1 |
| **H3-19-0.5%** | 0.5 | 0.25 | 0.25 | 1 |

*Mix symbol-Fiber length-long fibre content

## 2.2. Laboratory testing

### 2.2.1. Compressive strength test

The compressive strength was prepared and tested in accordance with ASTM C39 [24]. Cylinder samples with dimensions of 200 mm x 100 mm were used to measure the compressive strength and uniaxial compressive load-displacement curve. Two specimens were tested at 28 days, and results were recorded. Load and deformation values were captured through a data acquisition system. Two linear variable differential transformers (LVDTs) were installed on each side of the specimens to measure the deformation. Figure 3 shows the testing machine.

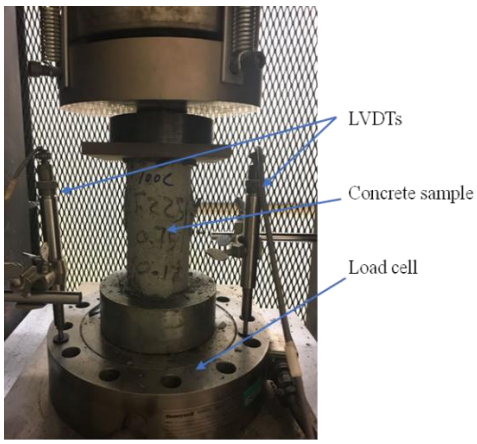


**Fig. 3. Compressive strength test setup.**

### 2.2.2. Direct tensile test method

Many methods were employed to evaluate the direct tensile strength of the concrete because the ASTM did not define a standard approach for testing the direct tensile

strength of concrete. However, all the previous methods had experienced testing issues related to nonuniform failure planes or concentrated stresses [25]. Therefore, the current method is designed to address the test's previous issues.

The new direct tensile test utilized a cylindrical specimen with a length of 150 mm and a diameter of 75 mm. The specimen was linked in the machine testing with two steel nipples and two steel caps, as shown in Fig. 4. The steel nipples were glued to concrete specimens. The elongation of the specimens was measured using LVDT. To ensure a uniform stress distribution in the middle of the concrete specimen, a notch was created at its centre. A finite element model, created using Abaqus software, was developed to determine the optimal notch depth. For steel parts, the elastic modulus of and Poisson's ratio defined in the Abaqus model were 200 GPa and 0.3, respectively.

For fibre reinforced concrete, the model of concrete damage plasticity (CDP) was used to define the concrete material because it is capable of simulating the nonlinear behaviour of concrete. The CDP model assumes that concrete fails through two primary mechanisms: cracking under tension and crushing under compression. Compressive and tensile stress-strain curve of the mix design H1 was defined in the FEM. The CDP includes five parameters are shown in Table 3. After several attempts, the notch with a depth of 6.35 mm was chosen. Figure 5 illustrates the deformation that developed in the notched area.

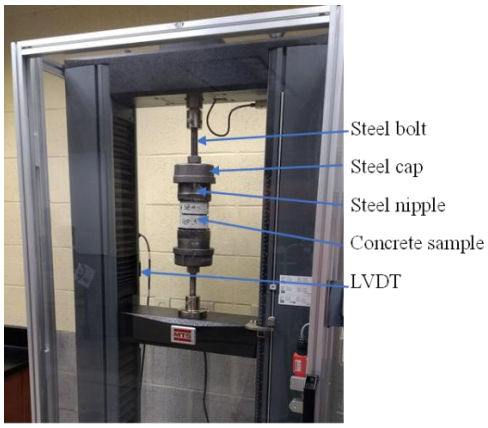


**Fig. 4. Direct tension test setup.**

**Table 3. CDP Properties used for slag concrete mix H1.**

| Property | Magnitude |
|---|---|
| **Compressive strength (MPa)** | 61 |
| **Modulus of elasticity (GPa)** | 36.7 |
| **Poisson's ratio** | 0.2 |
| **CTE (x10$^{-6}$/$^{o}$C)** | 12.7 |
| **dilation angle in degrees (ψ)** | 36.67$^{o}$ |
| **flow potential eccentricity (ϵ)** | 0.1 |
| **Kc** | 0.67 |
| **viscosity parameter (μ)** | 0.001 |
| **σb0/σc0** | 1.16 |

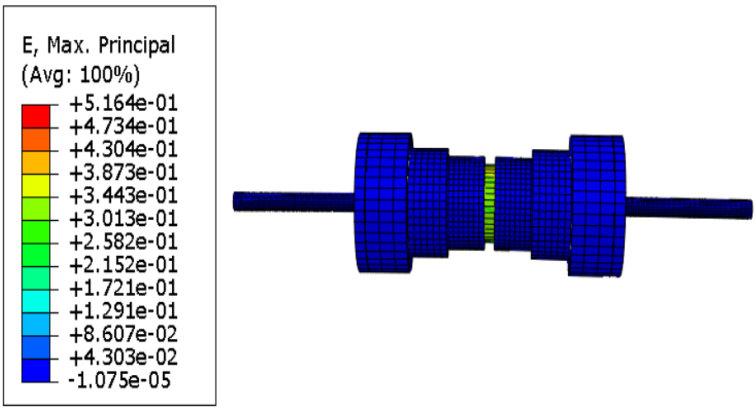


**Fig. 5. Tensile strain distributed at the mid-height.**

### 2.2.3. Coefficient of thermal expansion test

The coefficient of thermal expansion (CTE) of slag concrete specimens was determined using the Ohio CTE Device (OCD), designed to determine the thermal contraction (CTC) of asphalt mixes and later adapted for measuring the CTE of concrete. The OCD was employed to address the limitations of AASHTO TP60-00 [26], CRD 39 [27], and ASTM C531 [28] by functioning across a temperature range of 60 °C to -60 °C under air dry conditions to investigate extreme temperature effects on the CTE of concrete [29, 30].

Figure 6 depicts the OCD and the specimen mounted in the chamber. Additional information regarding the OCD is provided by Kim et al. [29].

Before testing, the apparatus was carefully calibrated with an invar cross square, and the measurement system was verified using stainless steel discs and aluminium 6061, in accordance with the procedures outlined by Kim et al. [29].

The CTE specimens were cast in cylindrical moulds measuring 150 × 300 mm. After 28 days, they were cut into slices of 25 × 150 mm and dried for 48 hours at room temperature to minimize moisture effects before being tested in the OCD.

The slag concrete specimens were tested at 28 days and exposed to thermal cycles ranging from 60 ºC to -60 ºC. The thermal cycle began with a controlled heating stage in which the chamber temperature increased from ambient conditions to 60 °C within 1 h.

This temperature was then maintained for 1 h to ensure uniform thermal conditioning of the specimen. Subsequently, the temperature was gradually reduced from 60 °C to -60 °C over a 6 h period, imposing a sustained cooling phase and subjecting the specimen to a substantial thermal gradient.

After reaching -60 °C, the temperature was held constant for 1 h to allow stabilization under the low-temperature condition. Finally, the chamber temperature was increased from -60 °C back to 60 °C over 6 h, thereby completing the full heating-cooling-heating cycle. The temperature variation applied during testing is illustrated in Fig. 7.


**Fig. 6. Ohio CTE device.**

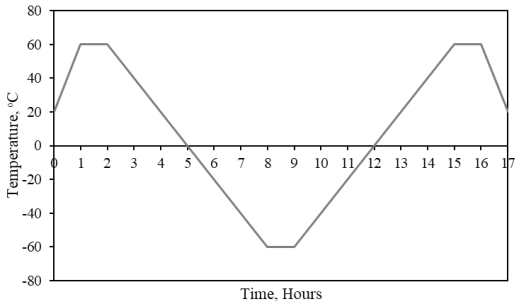


**Fig. 7. Temperature variation used in the test.**

## 3. Results and Discussion

### 3.1. Compressive load-displacement curve

Figure 8 depicts the load-displacement curve for the slag concrete specimen tested at 28 days, and the compressive strength values are given in Table 4. The inclusion of hybrid PP fibres had a minimal influence on the elastic-linear behaviour of the slag concrete mixtures, but their post-cracking response can be significantly modified. All the tested specimens exhibit a linear segment until the ultimate load, after which a gradual decrease in load occurs. The average of the failure load of control specimen C was 538 kN. The average of the failure load of specimens H1, H2, and H3 was 482, 474, and 461 kN, respectively. Based on the tested specimens, the ultimate failure load of the control specimen was higher than that of all the specimens with fibre. It is indicated that the hybrid PP fibre had a slight effect on the ultimate failure load.

One of the main issues with PP fibres in concrete is their tendency to clump together and form voids around the fibres. This behaviour can lead to weak zones within the matrix, ultimately reducing the compressive strength of the concrete [31, 32]. However, the compressive strength of H1 was 10% and 15% higher than that of H2 and H3, respectively. It is clear that slag concrete mixtures with fibre exhibit a compressive load-displacement curve with a similar ascending segment but a different descending segment, which is characterized by a lower slope compared to that of a non-fibrous mixture. This behaviour indicates that slag concrete without fibre exhibited a more brittle failure compared to that with fibre. Longer fibres enhanced the post-cracking ductility and increased the toughness of the concrete, as indicated by a larger area beneath the load-displacement curve.

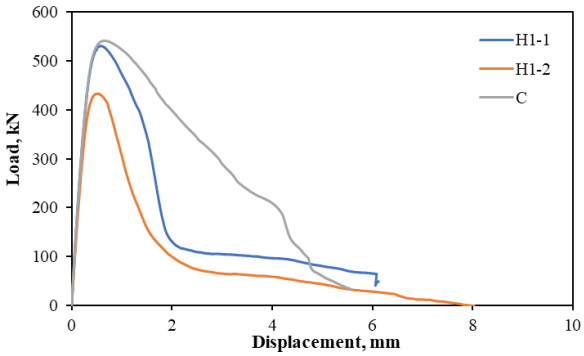


**(a)**

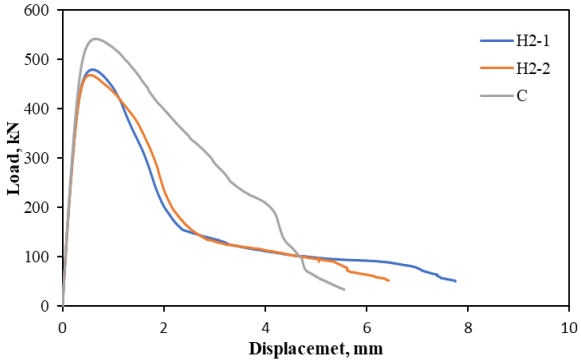


**(b)**

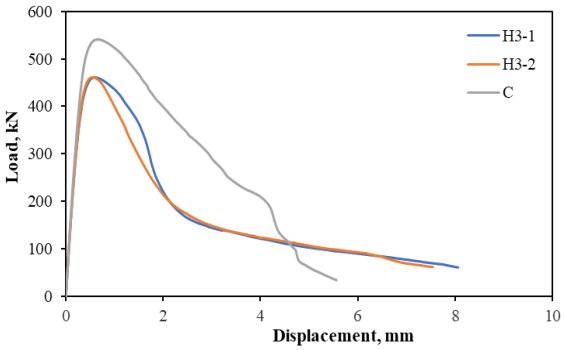


**(c)**

**Fig. 8. Load-displacement curve for slag concrete, (a) Mix H1 vs. Mix C, (b) Mix H2 vs. Mix C, (c) Mix H3 vs. Mix C.**

**Table 4. Results of compressive strength (MPa).**

| Mix | Sample 1 | Sample 2 | Average |
|---|---|---|---|
| **C** | 68 | 68 | 68 |
| **H1-57-0.5%** | 67 | 55 | 61 |
| **H2-38-0.5%** | 61 | 60 | 60.5 |
| **H3-19-0.5%** | 59 | 59 | 59 |

### 3.2. Direct tension results

The direct tensile strength was investigated at 28 days. Figure 9 illustrates the axial tensile load-deflection curve of slag concrete specimens. As expected, the failure mode for all specimens occurred at the midpoint of the specimen height as shown in Fig. 10. The consistency of the results was attributed to the optimized notch geometry and the effectiveness of the test setup in providing a uniform stress distribution in the central region of the specimens. This behaviour indicates that the newly developed direct tension test minimizes stress eccentricity, thereby greatly improving the reliability of the experimental outcomes. The load-displacement relationship was linear until it reached its ultimate value, after which it decreased suddenly due to the rapid load rating of the testing machine.

Based on the tested specimens, the ultimate tensile load for C, H1, H2, and H3 was 12.7, 15.22, 14.69, and 14.23 kN, respectively. The maximum displacements for C, H1, H2, and H3 were 1.69, 1.65, 1.53, and 1.42 mm, respectively. The maximum tensile strength of the control specimens was 3.66 MPa, whereas the maximum tensile strengths of H1, H2, and H3 were 4.43, 4.24, and 4.14 MPa, respectively. It can be noted that the ultimate tensile strength can be increased by 17%, 14%, and 12% corresponding to PP fibre contents of 1%. The results demonstrate that hybrid PP fibres affect the tensile strength of slag concrete. The inclusion of a high volume of long fibres in the mix had an apparent influence on the ultimate tensile strength. Mixture H1, containing a higher fibre content of 0.5% with a fibre length of 57 mm, exhibited increased ultimate tensile strength. This behaviour is attributed to the fact that the percentage of longer fibres provides stronger bonding and exhibits improved behaviour after cracking compared to shorter ones.

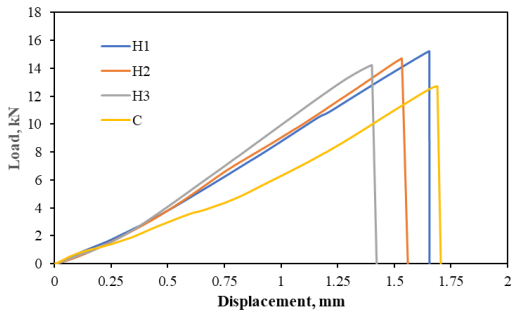


**Fig. 9. Load-displacement curves of slag concrete made with hybrid PP fibres.**

**Fig. 10. Failure mode.**

### 3.3. Coefficient of thermal expansion results

Thermal stresses significantly affect the performance of concrete bridge slabs, which may develop transverse cracking when restrained from movement. These stresses are influenced by temperature fluctuations, the coefficient of thermal expansion, and the modulus of elasticity. These factors mainly affect the aggregate type, which represents approximately 75% of the concrete volume [30]. Therefore, the evaluation of thermal stress and the coefficient of thermal expansion (CTE) in slag concrete plays a substantially important role in the long-term performance of concrete bridge slabs.

The performance of the slag concrete mixes under temperature cycles was assessed. Figure 11 depicts the behaviour of thermal strain versus temperature condition for both fibre and plain slag concrete. It was observed that all the slag concrete mixes experience a linear change in strain versus temperature, ranging from 60 oC to -60 oC. The maximum and minimum strains are tabulated in Table 5. It was observed that incorporating hybrid PP fibres into slag concrete increases thermal strain, especially at a temperature of -60 °C.

The maximum increase in thermal strain under a temperature of -60 °C compared to the control mix was 25%, 14%, and 15% for mixes H1, H2, and H3, respectively. The findings of this study agreed with the findings of a previous study [33], which reported that the thermal strain of PP fibre concrete is higher than that of plain concrete.

The coefficient of thermal expansion (CTE) is determined by the slope of the linear portion of the thermal strain-temperature curve. Table 6 presents the CTE value of the slag concrete mixes. The CTE value over the heating and cooling cycle was found to be 11.91 $10^{-6}$/°C, 12.7 $10^{-6}$/°C, 13.0 $10^{-6}$/°C, and 13.7 $10^{-6}$/°C for mixes C, H1, H2, and H3, respectively. The CTE value of the mix C at 28 days was slightly lower than that of fibrous slag concrete. The CTE value of the C was 6%, 8%, and 13% lower than that of H1, H2, and H3 mixes, during the cooling and heating cycle from 60 °C to -60 °C, respectively.

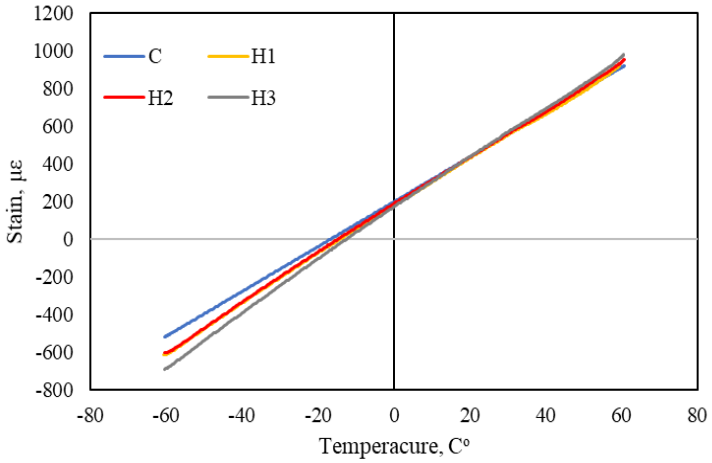


**Fig. 11. Thermal strain of slag concrete.**

**Table 5. Maximum and minimum strain.**

| Mix ID | Maximum strain, με | Minimum strain, με |
|---|---|---|
| **C** | 921 | -521 |
| **H1** | 922 | -616 |
| **H2** | 955 | -605 |
| **H3** | 983 | -691 |

**Table 6. Coefficient of thermal expansion results for temperature from -60 to 60°C.**

| Mix ID | CTE ($10^{-6}$/°C) |
|---|---|
| **C** | 11.91 |
| **H1** | 12.7 |
| **H2** | 13.0 |
| **H3** | 13.7 |

## 3.4. Analysis of test results

### 3.4.1. Toughness measurements

The toughness, referring to the amount of energy concrete can absorb under loading until failure, was utilized to evaluate the effects of the hybrid PP fibres. The calculation of toughness was adopted from the ASTM C1018 [34]. The toughness of all the mixtures is presented in Fig. 12. The toughness of the C, H1, H2, and H3 was 9.55, 12.06, 10.59, and 9.63 N-m, respectively. It can be seen that incorporating hybrid PP fibre into the slag concrete mixes enhanced tensile toughness, thereby improving the concrete's resistance to cracking. Tensile toughness values generally increased when the slag concrete mix contains PP fibres, regardless of the length of the fibres. Moreover, the increase in tensile toughness is generally related to the percentage of fibre length in the mixes. H1 mix had a higher toughness value compared to the other mixes. In addition, the control mixture C and H3 had approximately similar toughness values. This is a logical consequence attributed to the lack of long fibres in the mix, as longer fibres provide stronger bonding and exhibit improved behaviour after cracking compared to shorter ones.

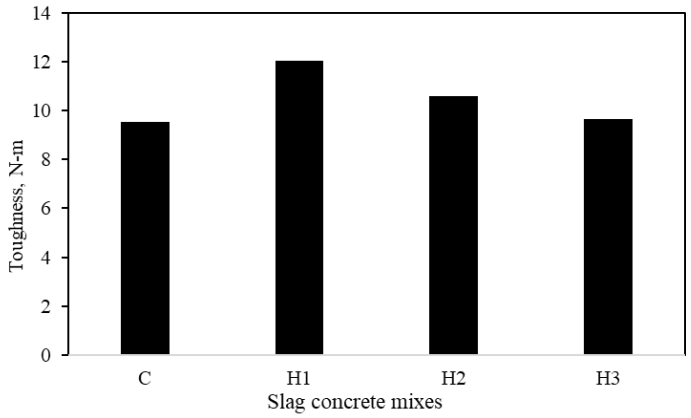


**Fig. 12. Concrete toughness.**

### 3.4.2. Modulus of elasticity calculation

The modulus of elasticity of slag concrete is a crucial property, indicating its stiffness and playing a crucial role in structural design. The modulus of elasticity is typically estimated using the linear portion of a stress-strain curve obtained during compressive strength testing. The elastic region was defined as 50% of the ultimate compressive strength. The initial part of the stress-strain curve is linear, indicating the elastic response of the concrete. If the fibre content is less than 2%, the modulus of elasticity is generally considered equal to that of a similar non-fibrous concrete [35]. Therefore, the experimental results were compared with the calculated values obtained from Equations (1) and (2) of the American Concrete Institute ACI 318 [36] and ACI 363R [37], respectively, for non-fibrous concrete. The comparison results are summarized in Table 7. A good agreement was observed between the results from the ACI 318 [36] equation and the experimental data. The maximum deviation between the ACI 318 [36] results and the experimental results was 5%, whereas the deviation between the ACI 363 [37] results and the experimental results was 15%. Also, it was observed that the ACI 318 [36] equation results are lower than the experimental results. This behaviour indicates that the ACI 318 [36] equation provides an overly conservative design approach for estimating modulus of elasticity for both fibrous and non-fibrous slag concrete. Consequently, the ACI 318 [36] equation can be used to estimate the modulus of elasticity of slag concrete.

$$E = 4700*\sqrt{f'c} \quad (1)$$

$$E = 3320*\sqrt{f'c} + 6900 \quad (2)$$

The modulus of elasticity of the control mix is slightly higher than that of mixes with fibre. The modulus of elasticity of mix C was higher than that of mixes H1, H2, and H3 by 1%, 3%, and 5% respectively. The reduction in the magnitude of the modulus of elasticity indicates that the addition of hybrid PP fibre can enhance the ductility of the concrete. It was also noted that the incorporation of long PP fibres in slag concrete showed a trend toward improving its modulus of elasticity. Mix H1, containing 0.5% fibre with a length of 57 mm, exhibited a higher modulus of elasticity by 3% and 5% compared to the H2 and H3 mixes, respectively.

**Table 7. The comparison results of modulus of elasticity (MPa).**

| Concrete Mix | Experiment | ACI 318 [36] Equation | Deviation, % | ACI 363 [37] Equation | Deviation, % |
|---|---|---|---|---|---|
| **C** | 38865 | 38757 | 0.3 | 34277 | 12 |
| **H1** | 38534 | 36708 | 5 | 32830 | 15 |
| **H2** | 37720 | 36557 | 3 | 32724 | 13 |
| **H3** | 37006 | 36101 | 2 | 32401 | 12 |

## 3.5. Finite element results

### 3.5.1. Finite element model

The finite element model (FEM) for bridge which constructed on Route 271 in Mayfield Ohio was created using Abaqus version 6.14 software. The bridge consisted of two spans with total length of 58.25 m and width of 19.30 m. The bridge superstructure consisted of seven continuous W-shaped steel girders (1.00

m deep) spaced at 2.90 m, carrying a concrete deck 22 cm thick. The FEM was calibrated and validated under truck and thermal loading to investigate the performance of the bridge under truck and thermal loadings [30].

The model was consisted of several components of the superstructure, which include the concrete deck, reinforcing bars, the steel girders, the concrete diaphragms at the ends, the steel cross-fame diaphragms, and concrete barriers. All of the superstructure components, except the cross-frame diaphragm, were modelled using C3D8R three-dimensional linear brick elements with reduced integration was used to model all of the superstructure components, except the steel cross-frame diaphragm which was model as a B31 one-dimensional element. The mesh size for the steel girder and concrete deck was 5 inches, whereas the steel cross-frame diaphragm was divided to 14 elements. The interaction between the concrete deck and the steel girders was modelled as a full composite action because no slip was assumed at the interface.

In current study, material properties of the mix design H1 defined in the FEM are shown in Table 3. For steel parts, the elastic modulus of and Poisson's ratio, and the coefficient of thermal expansion were 200 GPa, 0.3, and 10 x$10^{-6}$/°C, respectively.

### 3.5.2. Parametric study

The calibrated and validated FEM was utilized to conduct parametric study to investigate the influence of temperature gradient on the behaviour of the slag concrete deck. The effect of temperature gradient on the slag concrete deck was investigated. The positive and negative temperature gradients throughout the bridge superstructure were defined according to AASHTO LRFD (2017) [38], which subdivides the U.S. into four zones. Zone 3 was selected for the FEM analysis because the state of Ohio is located within this zone. The temperature gradient profile for Zone 3 for a composite steel girder is shown in Fig. 13.

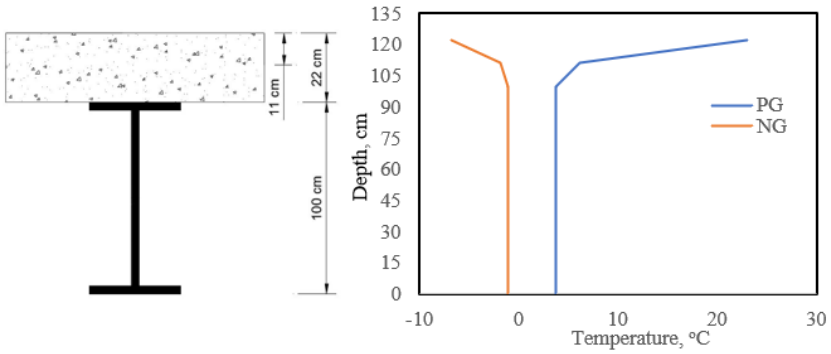


**Fig. 13. AASHTO LRFD temperature gradient for zone 3.**

The FEM results showed that the maximum tensile stress in the concrete deck caused by the positive temperature gradient was 4.10 MPa (590.8) psi, as shown in Fig. 14. This thermal stress is approximately 5% lower than the tensile strength of slag concrete which was 4.43 MPa. The temperature gradient induced longitudinal bending, which was constrained by the steel girders, resulting in the development of tensile

stresses in the deck [30]. This indicates that PP fibres generate higher thermal stresses in reinforced concrete members; however, they simultaneously help prevent thermal cracking and limit crack propagation within the concrete [39]. Under the negative temperature gradient, the maximum tensile stress in the deck was 1.65 MPa (239.6 psi) This stress is about 60% lower than the tensile strength of the concrete.

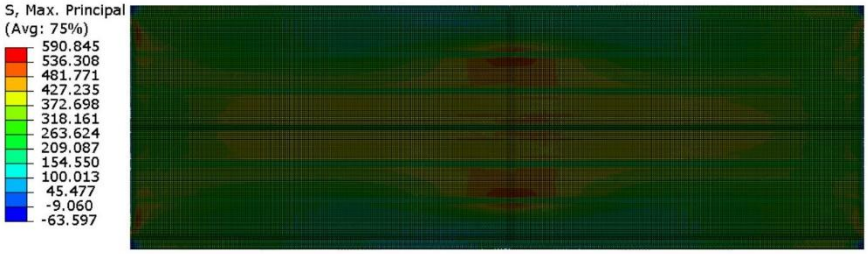


**(a)**

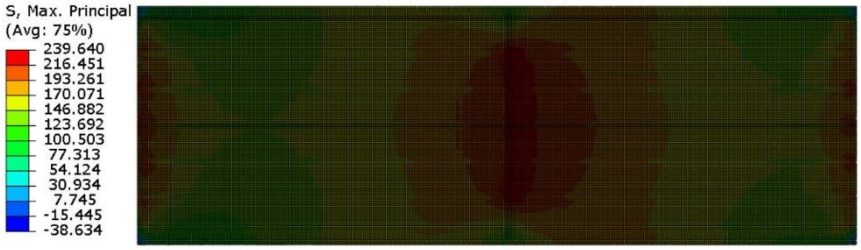


**(b)**

*The stresses are in psi. 1 MPa = 145 psi

**Fig. 14. Fiber reinforced deck stress (a) positive temperature gradient, (b) negative temperature gradient.**

## 4. Summary, Conclusion and Recommendations

The influence of incorporating slag aggregate on the strength performance of concrete was assessed. The concrete mixes included 100% coarse slag aggregates along with hybrid PP fibres. A new testing for tensile strength was employed to evaluate the concrete's structural capacity. Based on the findings, the following conclusions can be made:

- Incorporating hybrid PP fibre with slag concrete has an observed effect on mechanical properties.
- The newly developed direct tension test minimizes stress eccentricity, thereby significantly improving the reliability of the experimental outcomes.
- The incorporation of a higher volume of long fibres in the mix has an apparent influence on the ultimate tensile strength. This effect is primarily due to the superior bonding capacity and improved post-cracking performance of longer fibres compared to shorter ones.
- Tensile toughness typically improved with the inclusion of PP fibres in the slag concrete mixtures, regardless of fibre length. Additionally, the enhancement in tensile toughness was generally associated with the proportion of longer fibres in the mixes.

- The modulus of elasticity increased with increasing PP fibre length in the slag concrete mix. The incorporation of a higher amount of long PP fibres increased the modulus of elasticity by up to 5%.
- It was found that positive temperature gradient provides a higher thermal concrete stress compared with negative temperature gradient.

This study provides insights for designing hybrid PP fibre-reinforced slag concrete to achieve the desired mechanical performance for construction applications. However, the experimental program was limited to a specific range of fibre types and dosages. Future studies involving a broader range of hybrid PP fibre dosages are recommended to further validate and extend these findings. Additionally, further investigations should examine the economic benefits, durability, microstructural tests, and long-term performance of the hybrid PP fibre reinforced slag concrete.

## References

1. Brown, M.D.; Smith, C.A.; Sellers, J.G.; Folliard, K.J.; and Breen, J.E. (2007). Use of alternative materials to reduce shrinkage cracking in bridge decks. *ACI Materials Journal*, 104(6), 629-637.
2. Darwin, D.; Browning, J.; Lindquist, W.; McLeod, H.A.; Yuan, J.; Toledo, M.; Reynolds, D. (2010). Low-cracking, high-performance concrete bridge decks: Case studies over first 6 years. *Transportation Research Record*, 2202(1), 61-69.
3. Byard, B.E.; Schindler, A.K.; Barnes, R.W. (2012). Early-age autogenous effects in internally cured concrete and mortar. *ACI Special Publication*, 290, 1-18.
4. Hamid, W.K.; Steinberg, E.P.; Khoury, I.; Semendary, A.A.; Walsh, K. (2021). Thermally induced behavior of paired internally cured concrete and conventional concrete decks in composite bridges. *Journal of Bridge Engineering*, 26(4), 04021016.
5. Bentz, D.; Weiss, W.J. (2011). Internal curing: A 2010 state-of-the-art review. *National Institute of Standards and Technology* (*NISTIR*) *7765*, U.S. Department of Commerce, Washington, D.C. 82.
6. Krauss, P.D.; Rogalla, E.A. (1996). Transverse cracking in newly constructed bridge decks. *NCHRP Report 380*, Transportation Research Board of the National Academies, Washington, D.C.
7. Nevillle, A.M. (2011). *Properties of concrete*. (5th Ed.). Pearson Education, Harlow, UK.
8. Hamid, W.K.; Khoury, I.; Mandadapu, M.; Al Rikabi, F.T.; Ali, H. (2023). Evaluating the effect of incorporating slag cement with pre-wetted lightweight aggregate on reducing cracking of concrete bridge decks. *Advances in Civil Engineering Materials*, 12(1), 24-40.
9. Hamid, W.K.; Steinberg, E.P.; Semendary, A.A.; Khoury, I.; Walsh, K. (2020). Early-age behavior of internally cured concrete bridge deck under environmental loading. *Journal of Performance of Constructed Facilities*, 34(4), 04020066.
10. Dubey, S.; Singh, A.; Kushwah, S.S. (2019). Utilization of iron and steel slag in building construction. *AIP Conference Proceedings*, 2158(1), 020032.

11. US Geological Survey. (2022). Mineral commodity summaries. Iron and steel slag. Retrieved April 5, 2026, from https://pubs.usgs.gov/periodicals/mcs2022/mcs2022-iron-steel-slag.pdf
12. Guan, Q.; Xia, J.; Leng, F.; Zhou, Y. (2021). Utilizing blast furnace ferronickel slag as paste replacement to reduce white Portland cement content and improve performance of mortar. *Advances in Bridge Engineering*, 2(1), 18.
13. Latifi, M.R.; Biricik, Ö.; Aghabaglou, A.M. (2022). Effect of the addition of polypropylene fiber on concrete properties. *Journal of Adhesion Science and Technology*, 36(4), 345-369.
14. Al Rikabi, F.T.; Hussein, H.H.; Khoury, I.; Hamid, W.K.; Abdulmohsin, K.A. (2022). Structural performance of concrete corners reinforced with different steel reinforced detail under static loading. *Forensic Engineering*, 1109-1120.
15. Ortega-Lopez, V.; Garcia-Llona, A.; Revilla-Cuesta, V.; Santamaría, A.; San-Jose, J.T. (2021). Fiber-reinforcement and its effects on the mechanical properties of high-workability concretes manufactured with slag as aggregate and binder. *Journal of Building Engineering*, 43, 102548.
16. Al Rikabi, F.T.; Hussein, H.H.; Khoury, I. (2019). Experimental study on shear strength of synthetic fiber reinforced high-strength concrete containing slag aggregate. *Proceedings of Structures Congress 2019: Buildings and Natural Disasters*, American Society of Civil Engineers, Reston, VA, 179-187.
17. Zhao, W.; Liu, Z.; Wang, R. (2022). Effect of fibers on the mechanical properties and mechanism of cast-in-situ foamed concrete. *Advances in Materials Science and Engineering*, 2022(1), 2238187.
18. Qian, C.; Stroeven, P. (2000). Fracture properties of concrete reinforced with steel-polypropylene hybrid fibres. *Cement and Concrete Composites*, 22(5), 343-351.
19. Mehta, P.; Monteiro, P. (2014). *Concrete: Microstructure, properties, and materials*. McGraw-Hill Education, New York, USA.
20. He, F.; Biolzi, L.; Carvelli, V. (2022). Effect of fiber hybridization on mechanical properties of concrete. *Materials and Structures*, 55(7), 195.
21. Kinjawadekar, T.A.; Patil, S.; Nayak, G.; Kinjawadekar, A.; Kulal, S.A. (2024). Experimental study on mechanical properties of hybrid fiber-reinforced concrete. *Journal of Architectural Engineering*, 30(4), 06024001.
22. Khan, M.A.; Khan, Q.U.Z. (2025). Optimizing hybrid fiber concrete: An experimental analysis of steel and polypropylene fiber composites using RSM. *Materials Research Express*, 12, 025304.
23. Choi, Y.; Yuan, R.L. (2005). Experimental relationship between splitting tensile strength and compressive strength of GFRC and PFRC. *Cement and Concrete Research*, 35(8), 1587-1591.
24. ASTM C39. (2015). Standard test method for compressive strength of cylindrical concrete specimens. *ASTM International*, West Conshohocken, PA, USA.
25. Alhussainy, F.; Hasan, H.A.; Sheikh, M.N.; Hadi, M.N.S. (2019). A new method for direct tensile testing of concrete. *Journal of Testing and Evaluation*, 47(2), 704-718.

26. AASHTO TP60-00. (2000). Standard test method for the coefficient of thermal expansion of hydraulic cement concrete. *American Association of State Highway and Transportation Officials*, Washington, DC.
27. US Army Corps of Engineers. (1981). Test method for coefficient of linear thermal expansion of concrete. *Handbook for concrete and cement*. US Army Corps of Engineers, Washington, DC, USA.
28. ASTM C531. (2012). Standard test method for linear shrinkage and coefficient of thermal expansion of chemical-resistant mortars, grouts, monolithic surfacings, and polymer concretes. *ASTM International*. West Conshohocken, PA, USA.
29. Kim, S.S.; Nazzal, M.D.; Akentuna, M.; Abbas, A.R.; Arefin, M.S. (2015). Evaluation of low temperature cracking resistance of WMA. *No. FHWA/OH-2015/11*, Ohio Department of Transportation, Office of Statewide Planning & Research.
30. Hamid, W.K. (2020*). Behavior of bridge with internally cured concrete deck under environmental and truck loading*. Ph.D Thesis, Department of Civil Engineering, Ohio University.
31. Han, G.; Xiang, J.; Lu, S.; Zhou, Y.; Tang, Q.; Li, G.; Liu, Y. (2023). A review of microscopic characterization and related properties of fiber-incorporated cement-based materials. *Reviews on Advanced Materials Science*, 62(1), 20230341.
32. Akbulut, Z.F.; Kuzielová, E.; Tawfik, T.A.; Smarzewski, P.; Guler, S. (2024). Synergistic effects of polypropylene fibers and silica fume on structural lightweight concrete: analysis of workability, thermal conductivity, and strength properties. *Materials*, 17(20), 5042.
33. Al Rikabi, F.T.; Sargand, S.M.; Hussein, H.H.; Khoury, I. (2017). *The thermal expansion of synthetic fiber-reinforced concrete under air-dry and saturated conditions.* In *Congress on Technical Advancement*, 2017, Minnesota, US., 10-21.
34. ASTM C1018. (2010). Standard test method for flexural toughness and first-crack strength of fiber reinforced concrete (Using beam with third-point loading), *ASTM International*, West Conshohocken, PA, USA.
35. Daniel, J.I.; Gopalaratnam, V.S.; Galinat, M.A.; Ahmad, S.H.; Hoff, G.C.; Schupack, M.; Arockiasamy, M.; Jindal, R.L.; Shah, S.P.; and Balaguru, P.N. (2009). *544.1R-96*: *Report on fiber reinforced concrete*. ACI Committee 544.
36. ACI Committee 318. (2019). Building code requirements for structural concrete and commentary. *American Concrete Institute* (*ACI 318-19*), Farmington Hills, MI.
37. ACI Committee 363. (2010). Report on high-strength concrete. *American Concrete Institute* (*ACI 363R-10*), Farmington Hills, MI.
38. American Association of State Highway and Transportation Officials (AASHTO). (2017). AASHTO LRFD Bridge Design Specifications. Washington, DC.
39. Hejazi, S.M.; Abtahi, S.M.; Safaie, F. (2016). Investigation of thermal stress distribution in fiber-reinforced roller compacted concrete pavements. *Journal of Industrial Textiles*, 45(5), 896-914.